



Published in final edited form as:

*Cell Rep.* 2013 December 26; 5(6): 1489–1498. doi:10.1016/j.celrep.2013.11.041.

## Human natural killer cells prevent infectious mononucleosis features by targeting lytic Epstein-Barr virus infection

Obinna Chijioke<sup>1</sup>, Anne Müller<sup>1</sup>, Regina Feederle<sup>2</sup>, Mario Henrique M. Barros<sup>3</sup>, Carsten Krieg<sup>4</sup>, Vanessa Emmel<sup>5</sup>, Emanuela Marcenaro<sup>6</sup>, Carol S. Leung<sup>1</sup>, Olga Antsiferova<sup>1</sup>, Vanessa Landtwing<sup>1</sup>, Walter Bossart<sup>7</sup>, Alessandro Moretta<sup>6</sup>, Rocio Hassan<sup>5</sup>, Onur Boyman<sup>4</sup>, Gerald Niedobitek<sup>3</sup>, Henri-Jacques Delecluse<sup>2</sup>, Riccarda Capaul<sup>7</sup>, and Christian Münz<sup>1</sup>

<sup>1</sup>Viral Immunobiology, Institute of Experimental Immunology, University of Zurich, Zurich, Switzerland <sup>2</sup>DKFZ unit F100 / INSERM unit U1074, Heidelberg, Germany <sup>3</sup>Institute for Pathology, Unfallkrankenhaus Berlin, Berlin, Germany <sup>4</sup>Laboratory of Applied Immunobiology, University of Zurich, Zurich, Switzerland <sup>5</sup>Bone Marrow Transplantation Center, Instituto Nacional de Cancer (INCA), Rio de Janeiro, Brazil <sup>6</sup>Dipartimento di Medicina Sperimentale and Centro di Eccellenza per le Ricerche Biomediche, Università degli Studi di Genova, Genova, Italy <sup>7</sup>Institute of Medical Virology, University of Zurich, Zurich, Switzerland

### SUMMARY

Primary infection with the human oncogenic Epstein Barr virus (EBV) can result in infectious mononucleosis (IM), a self-limiting disease caused by massive lymphocyte expansion, which predisposes for the development of distinct EBV-associated lymphomas. It remains unclear why some individuals experience this symptomatic primary EBV infection, while the majority acquires the virus asymptotically. Using a mouse model with reconstituted human immune system components, we show here that depletion of human natural killer (NK) cells enhances IM symptoms and promotes EBV-associated tumorigenesis, mainly due to loss of immune control over lytic EBV infection. These data suggest that failure of innate immune control by human NK cells augments symptomatic lytic EBV infection, which drives lymphocyte expansion and predisposes for EBV-associated malignancies.

### Keywords

humanized mice; CD8<sup>+</sup> T cells; lymphoma; BZLF1; NKp46

---

Copyright © 2013 The Authors. Published by Elsevier Inc. All rights reserved.

Correspondence and requests for materials should be addressed to C.M. (christian.muenz@uzh.ch).

**Publisher's Disclaimer:** This is a PDF file of an unedited manuscript that has been accepted for publication. As a service to our customers we are providing this early version of the manuscript. The manuscript will undergo copyediting, typesetting, and review of the resulting proof before it is published in its final citable form. Please note that during the production process errors may be discovered which could affect the content, and all legal disclaimers that apply to the journal pertain.

### SUPPLEMENTAL INFORMATION

Supplemental Information contains Supplemental Experimental Procedures and Supplemental Figures 1–9.

### Author Contributions

O.C., A.M., M.H.M.B., G.N., C.S.L., R.H., C.K., V.E. and V.L. planned, performed and analyzed experiments. O.A. produced recombinant Epstein Barr virus stocks. W.B. and R.C. quantified viral titers. R.F., E.M., A.M., O.B., and H.J.D. provided crucial reagents. O.C. and C.M. designed the overall research and wrote the manuscript.

The authors declare no competing financial interests.

## INTRODUCTION

EBV is carried as a persistent infection by more than 90% of the human adult population (Young and Rickinson, 2004). While most individuals acquire the virus asymptotically, up to 10% develop IM, especially when primary infection is delayed into adolescence (Balfour et al., 2013; Kutok and Wang, 2006; Luzuriaga and Sullivan, 2010). This disease is accompanied by high EBV titers and massive lymphocytosis, primarily by EBV specific CD8<sup>+</sup> T cells targeting viral antigens that are involved in infectious particle production, called lytic infection (Hislop et al., 2007; Odumade et al., 2012). During the first 5 years after resolution of IM symptoms an increased risk to develop EBV-associated classical Hodgkin lymphoma is observed (Hjalgrim et al., 2003). EBV viremia, possibly driving EBV-specific CD8<sup>+</sup> T-cell expansion and tumorigenesis, could result from insufficient innate immune control of EBV, and indeed frequencies or counts for the innate lymphocytes natural killer (NK) cells were found to either inversely or directly correlate with EBV titers in infectious mononucleosis (Balfour et al., 2013; Williams et al., 2005). Further arguing for a role of NK cells in EBV-specific immune control, primary immunodeficiencies that affect NK cells or NK cell recognition of EBV-transformed B cells have been reported to be associated with EBV-positive malignancies and high susceptibility to EBV (Eidenschenk et al., 2006; Parolini et al., 2000; Shaw et al., 2012). Since experimental *in vivo* models to dissect the pathogenesis of this human B-cell tropic herpes-virus or close relatives are rare (Melkus et al., 2006; Sashihara et al., 2011; Traggiai et al., 2004; Yajima et al., 2008), it remained difficult to address and manipulate specific parameters of the immune response to EBV. In order to characterize the role of NK cells during primary EBV infection, we investigated NOD-scid  $\gamma_c^{-/-}$  mice with reconstituted human immune system components (huNSG mice), which constitute a suitable new *in-vivo* model for human NK cell responses and EBV infection as well as virus specific immune control (Ramer et al., 2011; Shultz et al., 2010; Strowig et al., 2010; Strowig et al., 2009; White et al., 2012; Yajima et al., 2009).

## RESULTS

### Human NK cells dampen immunophenotype during EBV infection

Human and mouse NK cells specifically express Nkp46 (Pessino et al., 1998; Walzer et al., 2007) and the majority of human NK cells of huNSG mice is positive for Nkp46 as well (Strowig et al., 2010). Therefore, the Nkp46 specific monoclonal antibody BAB281 was used for NK cell depletion. This treatment significantly diminished both CD3<sup>-</sup>Nkp46<sup>+</sup> and CD3<sup>-</sup>CD56<sup>+</sup> cell populations in treated mice (Figure S1 A and B), while an isotype control antibody did not alter the composition of the reconstituted human immune system compartments nor the course of infection (data now shown). Infection of huNSG mice via intraperitoneal inoculation with  $1 \times 10^5$  Raji infecting units (RIU) of B95-8 EBV resulted in increased CD8<sup>+</sup> T cells frequencies and total numbers in both spleen and blood over the 6-week course of infection (Figure 1 A–D). This characteristic feature of acute IM was significantly more pronounced in NK cell-depleted animals (Figure 1 A–D) and was accompanied with nearly tenfold elevated serum levels of IFN- $\gamma$  (Figure 1 E). Moreover, in animals depleted of human NK cells, IFN- $\gamma$  mRNA expressed in CD4<sup>+</sup> T cells was also significantly increased, reaching expression similar to CD8<sup>+</sup> T cells in non-depleted animals after infection (Figure 1 F and G). The splenomegaly, resulting from EBV-stimulated CD8<sup>+</sup> T cell expansion, was enhanced in the absence of NK cells (Figure 1 H). Thus, prominent features of symptomatic primary EBV infection in humans, i.e. acute IM, can be modeled in huNSG mice and are strongly pronounced in animals depleted of human NK cells.

### Human CD8<sup>+</sup> T cells display an activated memory phenotype after EBV infection

In order to characterize the IM-like T cell expansion after EBV infection of NK cell-depleted huNSG mice further, we phenotyped their CD4<sup>+</sup> and CD8<sup>+</sup> T cells. Activated memory T cells were mainly found within the CD8<sup>+</sup> T cell compartment in infected animals (Figure S2 A and B) and expanded at the cost of naïve CD8<sup>+</sup> T cell frequencies with NK cell depletion significantly affecting CX3CR1 up-regulation and expansion of CD11a<sup>+</sup>CD127<sup>-</sup>CD8<sup>+</sup> T cells, which in mice have been proposed to be short-lived effector cells (Kaech et al., 2003) (Figure S2 C and D). Inhibitory receptors and terminal differentiation markers on CD8<sup>+</sup> T cells were also significantly up-regulated upon EBV infection, exclusively on cells co-expressing the memory marker CD45RO (Figure S2 E). Still CD8<sup>+</sup> T cells displayed high levels of the effector molecules perforin and granzyme B with the latter significantly more expressed in animals depleted of NK cells (Figure S2 F). Despite this terminal differentiation phenotype of CD8<sup>+</sup> T cells during EBV infection of NK cell-depleted mice, these CD8<sup>+</sup> T cells were still able to exert considerable control over viral titers in NK cell-depleted animals, because CD8<sup>+</sup> T cell depletion on top of NK cell depletion led to one log increased viral loads in blood and spleen (Figure 1 I and J, for depletion efficiency see Figure S1 C and D). Thus, a highly activated, but still protective CD8<sup>+</sup> T cell phenotype that mimics the one seen in IM in humans (Hislop and Sabbah, 2008; Odumade et al., 2012) could be observed during EBV infection in huNSG mice, especially after human NK cell depletion.

### EBV infection drives an initial expansion of the human NK cell compartment

This NK cell-mediated restriction of CD8<sup>+</sup> T cell expansion was associated with the accumulation of a distinct NK cell subset in peripheral blood. We observed on average two-fold increased frequencies of NK cells (identified as CD3<sup>-</sup>NKp46<sup>+</sup> cells unless otherwise stated) four weeks post-infection (Figure 2 B and Figure S3 A), coinciding with increased CD16 expression on NK cells (Figure 2 C). This NK cell expansion or enhanced recruitment to the blood was followed by a contraction of NK cell frequencies in both the periphery and spleen (Figure 2 A and B and Figure S 3 A). Human NK cells six weeks post-infection did not significantly proliferate as indicated by staining for the proliferation marker Ki-67 (Figure S3 B) as has been described for NK cells in human acute IM (Zhang et al., 2007) and only slightly up-regulated the activation marker CD69 (Figure 2 E) compared to the robust up-regulation for both CD69 and Ki-67 on human CD8<sup>+</sup> T cells (Figure 2 E and Figure S3 B, respectively). Frequencies of more differentiated CD16<sup>+</sup> NK cells were still elevated (Figure 2 D), but the majority remained NKG2A positive and killer immunoglobulin-like receptor (KIR) negative (Figure 2 E and F). Nevertheless, NK cells expressed less CD27 and a subset up-regulated LIR-1 without increased expression of the terminal differentiation marker CD57 or NKG2C (Figure 2 E and F and data not shown). Therefore, EBV infection drives an initial NK cell accumulation in the blood that precedes the peak of the T cell response as well as a virus-induced lasting differentiation to mostly CD16<sup>+</sup>NKG2A<sup>+</sup>KIR<sup>-</sup> NK cells, indicative of an early differentiation phenotype.

### Human NK cells control viral load and prevent EBV-induced malignancy

The functional relevance of this NK cell subset accumulation became apparent from the analysis of viral titers in animals depleted of human NK cells. NK cells control EBV infection in huNSG mice, because cell-associated viral titers in both spleen and blood were increased one log five to six weeks post-infection in the absence of NK cells (Figure 3 A and B). Infected animals depleted of NK cells showed a dramatic loss of body weight (Figure 3 C) as well as a significantly higher incidence of infiltrative lymphomatous tumors at multiple sites (Figure 3 D–K and Figure S4 A), which were mostly monoclonal (Figure S4 B–D) compared to infected non-depleted animals. However, when NK cells were further expanded and differentiated to express CD16, KIRs and CD57 through cytokine-treatment

driven expansion and differentiation, they controlled EBV infection less well (Figure S5). These data indicate that especially human NK cells with an early differentiation phenotype control viral load and prevent detrimental cancerous sequelae of infection in the host.

### Human NK cells primarily respond to lytic EBV infection

Since during IM primarily lytic EBV antigen specific CD8<sup>+</sup> T cells expand (Hislop et al., 2007), the differential regulation of latent, i.e. cell proliferation inducing, versus lytic viral replication by NK cells was analyzed. Intriguingly, viral copy numbers in plasma of NK cell-depleted animals were more dramatically increased than in whole blood, up to 100-fold five and six weeks post-infection (Figure 4 A). This led us to investigate whether signs of lytic infection were more readily observed in the absence of NK cells. Indeed, BZLF-1 – one of the two immediate early trans-activators of EBV lytic cycle induction and indicator of lytic infection – and the late lytic antigen VCA p40 were expressed at increased levels in spleen sections from NK cell-depleted animals (Figure 4 B). Consistent with a higher availability of lytic EBV antigens, splenocytes of NK-cell depleted and infected animals recognized latently EBV infected autologous B cell lines (LCLs) significantly less well by IFN- $\gamma$  production than non-depleted controls (Figure 4 C), and some mice carried slightly elevated CD8<sup>+</sup> T cell populations that stained with MHC class I dextramers carrying lytic EBV antigen derived peptides (Figure S6). To confirm targeting of lytic infection by NK cells *in vitro*, we used AKBM cells that can be induced to enter the lytic cycle (Figure 4 D). As reported, lytic AKBM cells showed decreased expression of MHC class I molecules (Pappworth et al., 2007) (Figure 4 E) and as a surrogate for cytotoxicity elicited more degranulation of NK cells derived from EBV infected animals than latent AKBM cells (Figure 4 F). This preferential recognition of lytically EBV replicating B cells had been previously described for peripheral blood human NK cells *in vitro* (Pappworth et al., 2007). Together, these data suggest that NK cells preferentially respond to lytically infected cells and one reason for this might be loss of inhibitory signals delivered by MHC class I molecules on the target cells.

### Latent EBV infection is unaffected by human NK cells

To test our hypothesis that NK cell preferentially restrict lytic EBV infection *in vivo*, we infected animals with  $1 \times 10^5$  RIU BZLF-1 knock-out (KO) B95-8 virus, which is unable to switch to lytic replication and therefore can only establish the default program of latent EBV infection. Indeed, no significant weight loss or difference in tumor formation was observed after KO virus infection, irrespective of the presence or absence of NK cells (Figure 5 A and B). Viral titers in whole blood (Figure 5 C) and spleen (Figure 5 D) were not significantly affected by NK cell depletion six weeks post-infection. In contrast, a revertant virus, in which BZLF-1 was reinserted into the BZLF-1 KO EBV, replicated to higher blood and splenic viral titers in the absence of NK cells (Figure S7), and, therefore, behaved similar to the wild-type virus infection. Interestingly, immunoactivation of the T cell compartment and development of splenomegaly after BZLF-1 KO EBV infection was almost similar to wild-type EBV infection for both NK cell-depleted and non-depleted animals (Figure S8), confirming the potency of the KO virus. However, while a significant reduction of NK cells six weeks post-infection could still be observed in blood (Figure S9 A and B), KO virus infection failed to induce peripheral NK cell accumulation four weeks post-infection (Figure S9 B), nor did it elicit increases in differentiated CD16<sup>+</sup> NK cells (Figure S9 C and D). These results indicate an absence of protective NK cell responses to latent infection *in vivo*, and establish lytic infection as the main stimulus for NK cell accumulation and differentiation.

## DISCUSSION

Our study suggests that loss of NK cell-mediated immune control over lytic EBV infection allows this human tumor virus to replicate to higher titers, driving lymphocytosis and promoting predisposition for EBV-associated lymphoma development. These are IM-like symptoms and known sequelae of IM (Hjalgrim et al., 2003), and the monoclonality of the emerging tumors as well as the associated weight loss argue for manifestations of fatal IM (Brown et al., 1986; Wick et al., 2002). NK cells might act only late during the course of infection in our model, because EBV first establishes default latent infection of B cells after intraperitoneal injection. Lytic replication is then only later reactivated from this latent pool to produce virus particles for increased B cell transformation and/or conditioning of the microenvironment for tumor growth (Hong et al., 2005; Ma et al., 2011). Only this delayed lytic replication seems to be restricted by human NK cells in huNSG mice. Such continuous contributions of NK cell responses to viral immune control, in addition to their role during early immune restriction of viruses, have also been suggested to form the basis for the selective NK cell subset expansions, seen during hantavirus, human immunodeficiency virus (HIV), chikungunya virus and human cytomegalovirus (HCMV) infections (Bjorkstrom et al., 2011; Guma et al., 2004; Hong et al., 2010; Lopez-Verges et al., 2011; Petitdemanget et al., 2011). These expansions might result from restimulation of NK cells with immunological memory features (Paust et al., 2010; Sun et al., 2009) or from recruitment of NK cell subsets to immune responses by memory CD4<sup>+</sup> T cells (Bihl et al., 2010; Horowitz et al., 2010). Our data support such a prolonged immune control by NK cells during viral infections and suggest that human NK cells of an early differentiation phenotype selectively restrict lytic EBV replication.

Instead of CD8<sup>+</sup> T cell expansion by elevated viral titers, caused by uncontrolled lytic replication, human T cell expansion could, however, also result from loss of direct NK cell cytotoxicity towards activated T cells, as has been suggested in mice (Lang et al., 2012; Waggoner et al., 2012). In favor of this interpretation, we also observed, albeit weaker T cell expansion upon BZLF-1 knock-out virus infection in NK cell- depleted huNSG mice, without significant changes in EBV viremia. Therefore, NK cells might be involved in the prevention of IM by limiting viral antigen load that would otherwise drive massive T cell expansion and by restricting anti-viral T cell expansion directly via cytotoxic restriction of activated T cells - in a possibly perforin-dependent manner - as has been previously reported (Lang et al., 2012; Waggoner et al., 2012). These two scenarios do not need to be mutually exclusive but might indeed complement each other. Altogether, these data suggest that low NK cell reactivity – as shown for the association with increased cancer risk (Imai et al., 2000) - might identify EBV seronegative individuals at risk to develop IM, for which EBV vaccination could be developed.

## EXPERIMENTAL PROCEDURES

### Mice

NOD/LtSz-scid IL2R $\gamma$ <sup>null</sup> (NOD-*scid*  $\gamma_c^{-/-}$  or NSG) and HLA-A2 transgenic NSG (NSG-A2) mice were obtained from the Jackson Laboratory and bred and maintained at the Institute of Experimental Immunology, University of Zurich, Switzerland, under specific pathogen-free conditions. Newborn NSG mice (1 to 5 days old) were irradiated with 1 Gy using a Cs source. 5 to 6 hours after irradiation, mice were injected intrahepatically with 1–2  $\times 10^5$  CD34<sup>+</sup> human hematopoietic progenitor cells derived from human fetal liver tissue obtained from Advanced Bioscience Resources. Preparation of human fetal liver tissue and isolation of human CD34<sup>+</sup> cells was done as described previously (Strowig et al., 2010; Strowig et al., 2009; White et al., 2012). Reconstitution of human immune system components in mice (huNSG) was analyzed 10–12 weeks after engraftment and again just

before the start of the experiments. Mice with more than 60% reconstitution of huCD45<sup>+</sup> human immune system components in the lymphocytes of peripheral blood were used in the described experiments (average 85% huCD45<sup>+</sup> cells of peripheral blood lymphocytes, 30% CD3<sup>+</sup> T cells of human lymphocytes, 60% CD19<sup>+</sup> B cells of human lymphocytes, 3% NK cells of human lymphocytes, 80% CD4<sup>+</sup> and 20% CD8<sup>+</sup> T cells of human T cells), were of the NSG strain unless otherwise stated, sex-matched and 12–18 weeks old at the start of the experiments. All animal protocols were approved by the cantonal veterinary office of the canton of Zurich, Switzerland (protocol nos. 116/2008 and 148/2011). All studies involving human samples were reviewed and approved by the cantonal ethical committee of Zurich, Switzerland (protocol no. KEK-StV-Nr.19/08).

### Virus infection, NK and CD8<sup>+</sup> T cell depletion

GFP-Epstein-Barr virus (EBV) B95-8 wild-type, BZLF-1 KO and BZLF-1 KO revertant were produced in 293 cells. Titration of viral concentrates was done on Raji cells in serial dilutions and calculated as Raji infecting units (RIU) using flow cytometric analysis of GFP-positive Raji cells 2 days after infection of cells. HuNSG mice were infected via intraperitoneal injection of  $1 \times 10^5$  RIUs with the respective viruses and followed for 6 weeks. Depletion of NK cells in huNSG mice was done via intraperitoneal injection of purified anti-NKp46 antibody (clone BAB281) in PBS on three consecutive days (total of 300µg per mouse). On the following day, depletion efficiency was determined in peripheral blood by flow cytometry (Figure S1 A and B) and animals were infected by inoculation via intraperitoneal injection of  $1 \times 10^5$  RIU EBV. CD8<sup>+</sup> T cells were depleted with purified anti-CD8 antibody (clone OKT-8, Bio X Cell) diluted in PBS via intraperitoneal injection on three consecutive days (total of 150µg per mouse) before infection and again two weeks post-infection every second day (50µg per mouse each application).

### Flow cytometry

All fluorescently labeled antibodies were purchased from BD Biosciences, BioLegend, Invitrogen and R&D Systems. Spleens were mechanically disrupted and filtered through a 70-µm cell strainer before separation of mononuclear cells on Ficoll-Paque™ gradients. Lysis of erythrocytes in whole blood was done with NH<sub>4</sub>Cl. Dextramer staining was performed according to manufacturer's instructions (Immudex). For intracellular staining, the Cytotfix/Cytoperm™ kit from BD Biosciences was used. Cell suspensions were stained with antibodies for 30min on ice, washed and analyzed on FACSCanto or LSR Fortessa cytometers (BD Biosciences). Analysis of flow cytometric data was performed with FlowJo software (Tree Star).

### Quantification of viral load

Total DNA from whole blood or plasma was extracted using the QIAmp Mini kit (QIAGEN) according to the manufacturer's instructions. Splenic tissue (5 – 15 mg) was processed using the QIAmp tissue kit (QIAGEN) according to the manufacturer's protocol. DNA was eluted in 50 µl Tris-EDTA and stored at 4°C. Quantitative analysis of EBV DNA was performed by a TaqMan® (Applied Biosystems) real-time PCR technique as described (Berger et al., 2001) with modified primers for the *Bam*HI W fragment (5'-CTTCTCAGTCCAGCGCGTTT-3' and 5'-TCTAGGGAGGGGGACCACTG-3') and the fluorogenic probe (5'-(FAM)-CGTAAGCCAGACAGCAGCCAATTGTCAG-(TAMRA)-3'). All PCRs were run on an ABI Prism 7700 Sequence Detector (Applied Biosystems) and samples analyzed in duplicates.

## ELISA

Detection of human IFN- $\gamma$  in serum from huNSG mice was performed with a human IFN- $\gamma$  ELISA kit (Mabtech) according to the manufacturer's instructions.

## Quantitative real-time PCR

Total RNA was extracted using the RNeasy micro kit (QIAGEN) according to the manufacturer's instructions. Complementary DNA was reverse transcribed using GoScript™ Reverse Transcription System (Promega). Primers and probes were predesigned Taqman Gene Expression Assays (Applied Biosystems, IFN- $\gamma$ : Hs00989291\_m1 and 18S: Hs99999901\_s1). Real-time PCR was performed on a CFX384 Touch™ Real-Time PCR Detection System (Bio-Rad) machine. All samples were run in triplicates and normalized using 18S expression level.

## AKBM cells and degranulation assay

EBV positive AKBM cells that express GFP upon switch from latent to lytic EBV replication were induced to enter the lytic cycle after ligation with F(ab) IgG. BZLF-1 and HLA class I expression was monitored after intracellular staining for BZLF-1 (BZ-1, Santa Cruz) and surface staining for HLA-ABC (w6/32), respectively. For the degranulation assay, splenic cell suspensions and induced (lytic) or non-induced (latent) AKBM cells were co-cultured at a ratio of 1:1 for 5 hours with addition of monensin after 1 hour and NK cells were then analyzed for expression of the degranulation marker CD107a.

## Statistical analysis

All data was analyzed with two-tailed Student's *t* test unless otherwise stated. A P value of <0.05 was considered statistically significant. Statistical analysis and generation of graphs was performed using Prism software (GraphPad Software).

## Supplementary Material

Refer to Web version on PubMed Central for supplementary material.

## Acknowledgments

We are grateful to Drs. Maïke Rensing, Emmanuel Wiertz and Martin Rowe for providing the AKBM cells, and Silvia Behnke of Sophistolabs for the histology in Supplemental Figure 4.

This work was supported by the National Cancer Institute (R01CA108609), the Sassella Foundation (10/02, 11/02 and 12/02), Cancer Research Switzerland (KFS-02652-08-2010), the Association for International Cancer Research (11-0516), KFSP<sup>MS</sup> and KFSP<sup>HLD</sup> of the University of Zurich, the Vontobel Foundation, the Baugarten Foundation, the EMDO Foundation, the Sobek Foundation, Fondation Acteria, Novartis and the Swiss National Science Foundation (310030\_143979 and CRSII3\_136241) to C. Münz. R. Hassan is a fellow of the CNPq/INCT (Brazil) (Grants CNPq 481294/2009-0; 573806/2008-0 and FAPERJ - E-26/110.432/2010). M.H.M Barros is supported by the Alexander von Humboldt Foundation. O. Chijioke is the recipient of a postdoctoral fellowship of the Deutsche Forschungsgemeinschaft (DFG, CH 723/2-1).

## REFERENCES

- Balfour HH Jr, Odumade OA, Schmeling DO, Mullan BD, Ed JA, Knight JA, Vezina HE, Thomas W, Hogquist KA. Behavioral, virologic, and immunologic factors associated with acquisition and severity of primary Epstein-Barr virus infection in university students. *J Infect Dis.* 2013; 207:80–88. [PubMed: 23100562]
- Berger C, Day P, Meier G, Zingg W, Bossart W, Nadal D. Dynamics of Epstein-Barr virus DNA levels in serum during EBV-associated disease. *J Med Virol.* 2001; 64:505–512. [PubMed: 11468736]

- Bihl F, Pecheur J, Breart B, Poupon G, Cazareth J, Julia V, Glaichenhaus N, Braud VM. Primed antigen-specific CD4<sup>+</sup> T cells are required for NK cell activation *in vivo* upon Leishmania major infection. *J Immunol.* 2010; 185:2174–2181. [PubMed: 20624944]
- Bjorkstrom NK, Lindgren T, Stoltz M, Fauriat C, Braun M, Evander M, Michaelsson J, Malmberg KJ, Klingstrom J, Ahlm C, Ljunggren HG. Rapid expansion and long-term persistence of elevated NK cell numbers in humans infected with hantavirus. *J Exp Med.* 2011; 208:13–21. [PubMed: 21173105]
- Brown NA, Liu C, Garcia CR, Wang YF, Griffith A, Sparkes RS, Calame KL. Clonal origins of lymphoproliferative disease induced by Epstein-Barr virus. *J Virol.* 1986; 58:975–978. [PubMed: 3701935]
- Eidenschek C, Dunne J, Jouanguy E, Fourlinnie C, Gineau L, Bacq D, McMahon C, Smith O, Casanova JL, Abel L, Feighery C. A novel primary immunodeficiency with specific natural-killer cell deficiency maps to the centromeric region of chromosome 8. *Am J Hum Genet.* 2006; 78:721–727. [PubMed: 16532402]
- Guma M, Angulo A, Vilches C, Gomez-Lozano N, Malats N, Lopez-Botet M. Imprint of human cytomegalovirus infection on the NK cell receptor repertoire. *Blood.* 2004; 104:3664–3671. [PubMed: 15304389]
- Hislop AD, Sabbah S. CD8<sup>+</sup> T cell immunity to Epstein-Barr virus and Kaposi's sarcoma-associated herpes virus. *Semin Cancer Biol.* 2008; 18:416–422. [PubMed: 19007888]
- Hislop AD, Taylor GS, Sauce D, Rickinson AB. Cellular responses to viral infection in humans: lessons from Epstein-Barr virus. *Annu Rev Immunol.* 2007; 25:587–617. [PubMed: 17378764]
- Hjalgrim H, Askling J, Rostgaard K, Hamilton-Dutoit S, Frisch M, Zhang JS, Madsen M, Rosdahl N, Konradsen HB, Storm HH, Melbye M. Characteristics of Hodgkin's lymphoma after infectious mononucleosis. *N Engl J Med.* 2003; 349:1324–1332. [PubMed: 14523140]
- Hong GK, Gulley ML, Feng WH, Delecluse HJ, Holley-Guthrie E, Kenney SC. Epstein-Barr virus lytic infection contributes to lymphoproliferative disease in a SCID mouse model. *J Virol.* 2005; 79:13993–14003. [PubMed: 16254335]
- Hong HS, Eberhard JM, Keudel P, Bollmann BA, Ballmaier M, Bhatnagar N, Zielinska-Skowronek M, Schmidt RE, Meyer-Olson D. HIV infection is associated with a preferential decline in less-differentiated CD56<sup>dim</sup> CD16<sup>+</sup> NK cells. *J Virol.* 2010; 84:1183–1188. [PubMed: 19906929]
- Horowitz A, Newman KC, Evans JH, Korbel DS, Davis DM, Riley EM. Cross-talk between T cells and NK cells generates rapid effector responses to Plasmodium falciparum-infected erythrocytes. *J Immunol.* 2010; 184:6043–6052. [PubMed: 20427769]
- Imai K, Matsuyama S, Miyake S, Suga K, Nakachi K. Natural cytotoxic activity of peripheral-blood lymphocytes and cancer incidence: an 11-year follow-up study of a general population. *Lancet.* 2000; 356:1795–1799. [PubMed: 11117911]
- Kaech SM, Tan JT, Wherry EJ, Konieczny BT, Surh CD, Ahmed R. Selective expression of the interleukin 7 receptor identifies effector CD8 T cells that give rise to long-lived memory cells. *Nat Immunol.* 2003; 4:1191–1198. [PubMed: 14625547]
- Kutok JL, Wang F. Spectrum of Epstein-Barr virus-associated diseases. *Annu Rev Pathol.* 2006; 1:375–404. [PubMed: 18039120]
- Lang PA, Lang KS, Xu HC, Grusdat M, Parish IA, Recher M, Elford AR, Dhanji S, Shaabani N, Tran CW, et al. Natural killer cell activation enhances immune pathology and promotes chronic infection by limiting CD8<sup>+</sup> T-cell immunity. *Proc Natl Acad Sci U S A.* 2012; 109:1210–1215. [PubMed: 22167808]
- Lopez-Verges S, Milush JM, Schwartz BS, Pando MJ, Jarjoura J, York VA, Houchins JP, Miller S, Kang SM, Norris PJ, et al. Expansion of a unique CD57<sup>+</sup>NKG2C<sup>hi</sup> natural killer cell subset during acute human cytomegalovirus infection. *Proc Natl Acad Sci U S A.* 2011; 108:14725–14732. [PubMed: 21825173]
- Luzuriaga K, Sullivan JL. Infectious mononucleosis. *N Engl J Med.* 2010; 362:1993–2000. [PubMed: 20505178]
- Ma SD, Hegde S, Young KH, Sullivan R, Rajesh D, Zhou Y, Jankowska-Gan E, Burlingham WJ, Sun X, Gulley ML, et al. A new model of Epstein-Barr virus infection reveals an important role for

- early lytic viral protein expression in the development of lymphomas. *J Virol.* 2011; 85:165–177. [PubMed: 20980506]
- Melkus MW, Estes JD, Padgett-Thomas A, Gatlin J, Denton PW, Othieno FA, Wege AK, Haase AT, Garcia JV. Humanized mice mount specific adaptive and innate immune responses to EBV and TSST-1. *Nat Med.* 2006; 12:1316–1322. [PubMed: 17057712]
- Odumade OA, Knight JA, Schmeling DO, Masopust D, Balfour HH Jr, Hogquist KA. Primary Epstein-Barr virus infection does not erode preexisting CD8<sup>+</sup> T cell memory in humans. *J Exp Med.* 2012
- Pappworth IY, Wang EC, Rowe M. The switch from latent to productive infection in Epstein-Barr virus-infected B cells is associated with sensitization to NK cell killing. *J Virol.* 2007; 81:474–482. [PubMed: 17079298]
- Parolini S, Bottino C, Falco M, Augugliaro R, Giliani S, Franceschini R, Ochs HD, Wolf H, Bonnefoy JY, Biassoni R, et al. X-linked lymphoproliferative disease. 2B4 molecules displaying inhibitory rather than activating function are responsible for the inability of natural killer cells to kill Epstein-Barr virus-infected cells. *J Exp Med.* 2000; 192:337–346. [PubMed: 10934222]
- Paust S, Gill HS, Wang BZ, Flynn MP, Moseman EA, Senman B, Szczepanik M, Telenti A, Askenase PW, Compans RW, von Andrian UH. Critical role for the chemokine receptor CXCR6 in NK cell-mediated antigen-specific memory of haptens and viruses. *Nat Immunol.* 2010; 11:1127–1135. [PubMed: 20972432]
- Pessino A, Sivori S, Bottino C, Malaspina A, Morelli L, Moretta L, Biassoni R, Moretta A. Molecular cloning of Nkp46: a novel member of the immunoglobulin superfamily involved in triggering of natural cytotoxicity. *J Exp Med.* 1998; 188:953–960. [PubMed: 9730896]
- Petitdémange C, Becquart P, Wauquier N, Beziat V, Debre P, Leroy EM, Vieillard V. Unconventional repertoire profile is imprinted during acute chikungunya infection for natural killer cells polarization toward cytotoxicity. *PLoS Pathog.* 2011; 7:e1002268. [PubMed: 21966274]
- Rämer PC, Chijioke O, Meixlsperger S, Leung CS, Münz C. Mice with human immune system components as *in vivo* models for infections with human pathogens. *Immunol Cell Biol.* 2011; 89:408–416. [PubMed: 21301484]
- Sashihara J, Hoshino Y, Bowman JJ, Krogmann T, Burbelo PD, Coffield VM, Kamrud K, Cohen JI. Soluble rhesus lymphocryptovirus gp350 protects against infection and reduces viral loads in animals that become infected with virus after challenge. *PLoS Pathog.* 2011; 7:e1002308. [PubMed: 22028652]
- Shaw RK, Issekutz AC, Fraser R, Schmit P, Morash B, Monaco-Shawver L, Orange JS, Fernandez CV. Bilateral adrenal EBV-associated smooth muscle tumors in a child with a natural killer cell deficiency. *Blood.* 2012; 119:4009–4012. [PubMed: 22427204]
- Shultz LD, Saito Y, Najima Y, Tanaka S, Ochi T, Tomizawa M, Doi T, Sone A, Suzuki N, Fujiwara H, et al. Generation of functional human T-cell subsets with HLA-restricted immune responses in HLA class I expressing NOD/SCID/IL2r gamma<sup>null</sup> humanized mice. *Proc Natl Acad Sci U S A.* 2010; 107:13022–13027. [PubMed: 20615947]
- Strowig T, Chijioke O, Carrega P, Arrey F, Meixlsperger S, Ramer PC, Ferlazzo G, Münz C. Human NK cells of mice with reconstituted human immune system components require preactivation to acquire functional competence. *Blood.* 2010; 116:4158–4167. [PubMed: 20671122]
- Strowig T, Gurer C, Ploss A, Liu YF, Arrey F, Sashihara J, Koo G, Rice CM, Young JW, Chadburn A, et al. Priming of protective T cell responses against virus-induced tumors in mice with human immune system components. *J Exp Med.* 2009; 206:1423–1434. [PubMed: 19487422]
- Sun JC, Beilke JN, Lanier LL. Adaptive immune features of natural killer cells. *Nature.* 2009; 457:557–561. [PubMed: 19136945]
- Traggiai E, Chicha L, Mazzucchelli L, Bronz L, Piffaretti JC, Lanzavecchia A, Manz MG. Development of a human adaptive immune system in cord blood cell-transplanted mice. *Science.* 2004; 304:104–107. [PubMed: 15064419]
- Waggoner SN, Cornberg M, Selin LK, Welsh RM. Natural killer cells act as rheostats modulating antiviral T cells. *Nature.* 2012; 481:394–398. [PubMed: 22101430]

- Walzer T, Blery M, Chaix J, Fuseri N, Chasson L, Robbins SH, Jaeger S, Andre P, Gauthier L, Daniel L, et al. Identification, activation, and selective in vivo ablation of mouse NK cells via NKP46. *Proc Natl Acad Sci U S A*. 2007; 104:3384–3389. [PubMed: 17360655]
- White RE, Rämer PC, Naresh KN, Meixlsperger S, Pinaud L, Rooney C, Savoldo B, Coutinho R, Bödör C, Gribben J, et al. EBNA3B-deficient EBV promotes B cell lymphomagenesis in humanized mice and is found in human tumors. *J Clin Invest*. 2012; 122:1487–1502. [PubMed: 22406538]
- Wick MJ, Woronzoff-Dashkoff KP, McGlennen RC. The molecular characterization of fatal infectious mononucleosis. *Am J Clin Pathol*. 2002; 117:582–588. [PubMed: 11939733]
- Williams H, McAulay K, Macsween KF, Gallacher NJ, Higgins CD, Harrison N, Swerdlow AJ, Crawford DH. The immune response to primary EBV infection: a role for natural killer cells. *Br J Haematol*. 2005; 129:266–274. [PubMed: 15813855]
- Yajima M, Imadome K, Nakagawa A, Watanabe S, Terashima K, Nakamura H, Ito M, Shimizu N, Honda M, Yamamoto N, Fujiwara S. A new humanized mouse model of Epstein-Barr virus infection that reproduces persistent infection, lymphoproliferative disorder, and cell-mediated and humoral immune responses. *J Infect Dis*. 2008; 198:673–682. [PubMed: 18627269]
- Yajima M, Imadome K, Nakagawa A, Watanabe S, Terashima K, Nakamura H, Ito M, Shimizu N, Yamamoto N, Fujiwara S. T cell-mediated control of Epstein-Barr virus infection in humanized mice. *J Infect Dis*. 2009; 200:1611–1615. [PubMed: 19832115]
- Young LS, Rickinson AB. Epstein-Barr virus. 40 years on. *Nat Rev Cancer*. 2004; 4:757–768. [PubMed: 15510157]
- Zhang Y, Wallace DL, de Lara CM, Ghattas H, Asquith B, Worth A, Griffin GE, Taylor GP, Tough DF, Beverley PC, Macallan DC. *In vivo* kinetics of human natural killer cells: the effects of ageing and acute and chronic viral infection. *Immunology*. 2007; 121:258–265. [PubMed: 17346281]

**Article highlights**

- NK cell depletion leads to infectious mononucleosis features after EBV infection.
- Loss of NK cell mediated immune control leads to EBV-associated lymphomas.
- NK cells restrict only lytic EBV infection in humanized mice.

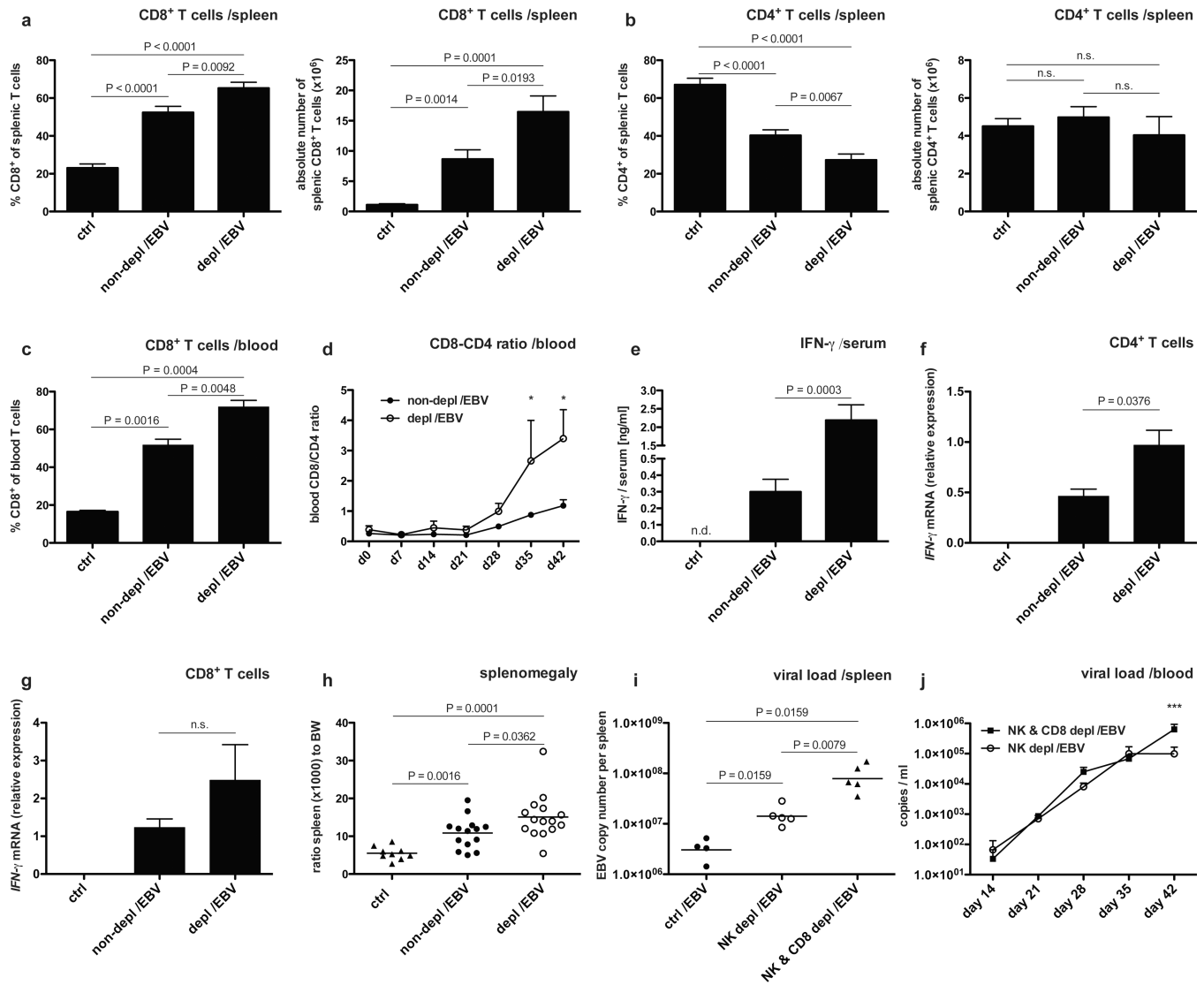


**Figure 1. Human NK cells curb human CD8<sup>+</sup> T cell expansion during EBV infection**

**a–d**, frequency and absolute numbers of CD8<sup>+</sup> T cells in spleen (**a**) and blood (**c**) six weeks after EBV infection in animals with (depl/EBV) and without (non-depl/EBV) NK cell depletion and in non-infected animals (ctrl). Frequency and absolute number of CD4<sup>+</sup> T cells in spleen six weeks p.i. (**b**) and CD8-CD4 ratio over time p.i. in blood (**d**, \*P<0.05, two-way analysis of variance (ANOVA) with Bonferroni correction). CD4<sup>+</sup> and CD8<sup>+</sup> T cells were identified within live huCD45<sup>+</sup>CD3<sup>+</sup> cells. n=9–34, mean  $\pm$  s.e.m. **e**, concentration of human IFN- $\gamma$  in serum six weeks p.i. in animals with and without NK cell depletion and in non-infected animals (n=18, mean  $\pm$  s.e.m.). **f–g**, relative expression of IFN- $\gamma$  mRNA normalized to 18S in CD4<sup>+</sup> T cells (**f**) and CD8<sup>+</sup> T cells (**g**) sorted from splenocytes of non-infected animals (ctrl), animals without (non-depl/EBV) and with NK cell depletion (depl/EBV) six weeks after EBV infection. Shown is one representative experiment of three independent experiments. n=8, mean  $\pm$  s.e.m. **h**, ratio spleen to body weight (BW) six weeks p.i. in animals with and without NK cell depletion and in non-infected animals (n=38, bar represents mean). Data represent composite data from two to four independent experiments. **i–j**, viral titers in spleen six weeks after EBV infection in animals without depletion (ctrl/EBV), animals depleted of NK cells (NK depl/EBV) and

animals depleted of both NK and CD8<sup>+</sup> T cells (NK & CD8 depl /EBV) (**i**, n=15, horizontal bar represents geometric mean, two-tailed Mann Whitney test) and (**j**) whole blood at various time points p.i. in animals depleted of both NK and CD8<sup>+</sup> T cells (NK & CD8 depl /EBV) and animals depleted of NK cells (NK depl /EBV) only (n=10–13 per time point, mean ± s.e.m., \*\*\*P<0.001, two-way analysis of variance (ANOVA) with Bonferroni correction). Data represent composite data from two independent experiments.

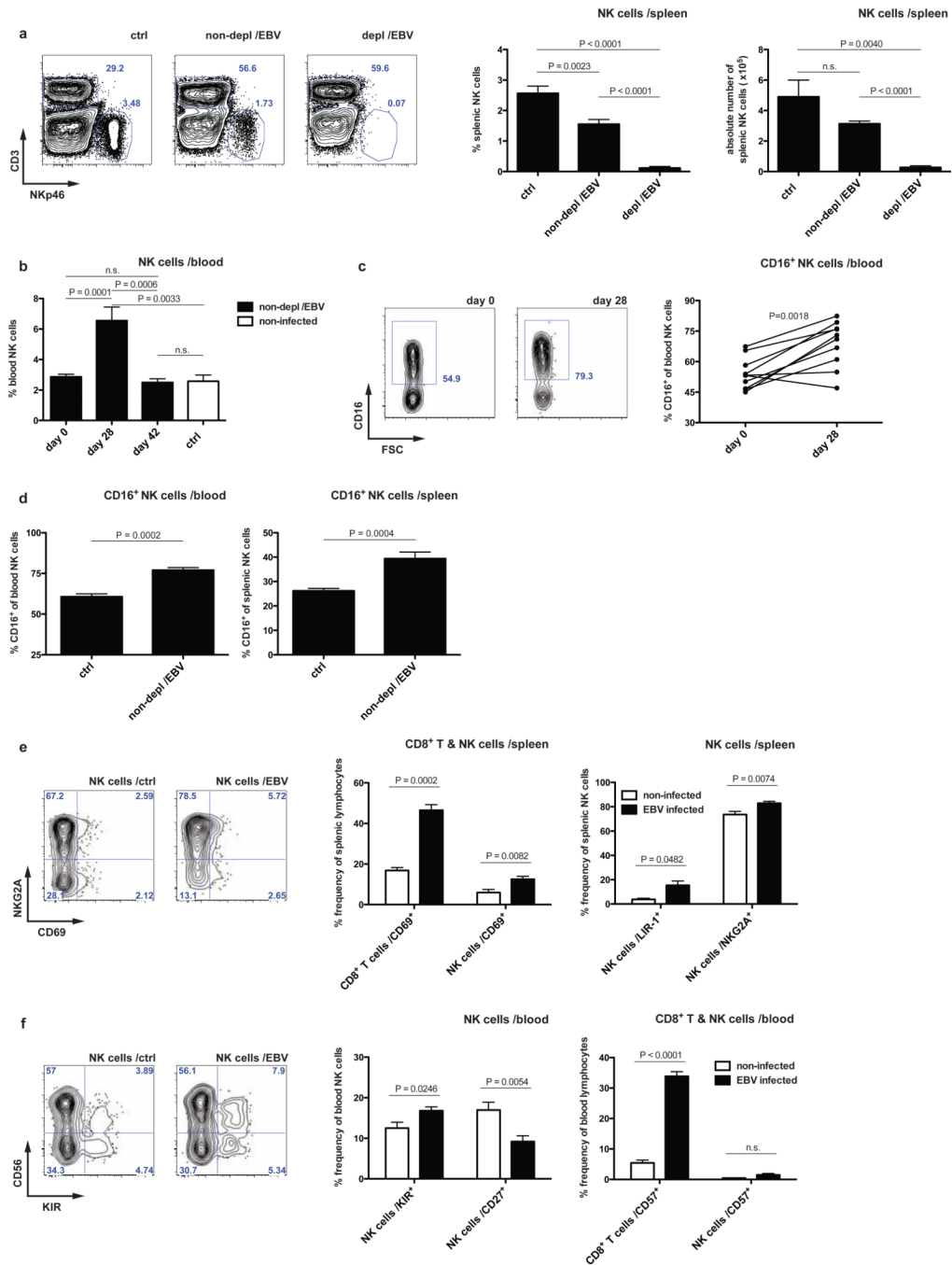


**Figure 2. EBV infection drives an initial expansion and an early differentiation phenotype of human NK cells**

**a.** frequency and number of splenic NK cells six weeks after EBV infection in animals with (depl /EBV) and without (non-depl /EBV) NK cell depletion and in non-infected animals (ctrl), respectively, with representative plots.  $n=22$ , mean  $\pm$  s.e.m. **b.** frequency of peripheral NK cells in non-depleted animals at day zero, day 28 p.i., day 42 p.i. and non-infected animals, respectively ( $n=27$ , mean  $\pm$  s.e.m.). **c.** expression of CD16 on peripheral NK cells in non-depleted EBV infected animals at day zero and day 28 p.i. ( $n=10$ ) with representative staining for CD16 on pre-gated NK cells. **d.** frequency of CD16<sup>+</sup> NK cells in blood and spleen six weeks p.i. in non-depleted animals ( $n=9$ , mean  $\pm$  s.e.m., one representative

experiment for spleen). **e–f**, expression of CD69 on splenic CD8<sup>+</sup> T cells and splenic NK cells, respectively and frequency of LIR-1<sup>+</sup> and NKG2A<sup>+</sup> splenic NK cells six weeks p.i. with representative staining for NKG2A vs. CD69 on pre-gated splenic NK cells six weeks p.i. (**e**). Frequency of KIR<sup>+</sup> and CD27<sup>+</sup> NK cells in peripheral blood with representative staining for CD56 vs. KIR on pre-gated peripheral NK cells and frequency of CD57<sup>+</sup> peripheral CD8<sup>+</sup> T or NK cells, respectively, six weeks p.i. (**f**). NK cells were identified as CD3<sup>-</sup> NKp46<sup>+</sup> cells within live huCD45<sup>+</sup> cells. n=9–17, mean ± s.e.m. Data represent composite data from two to four independent experiments.

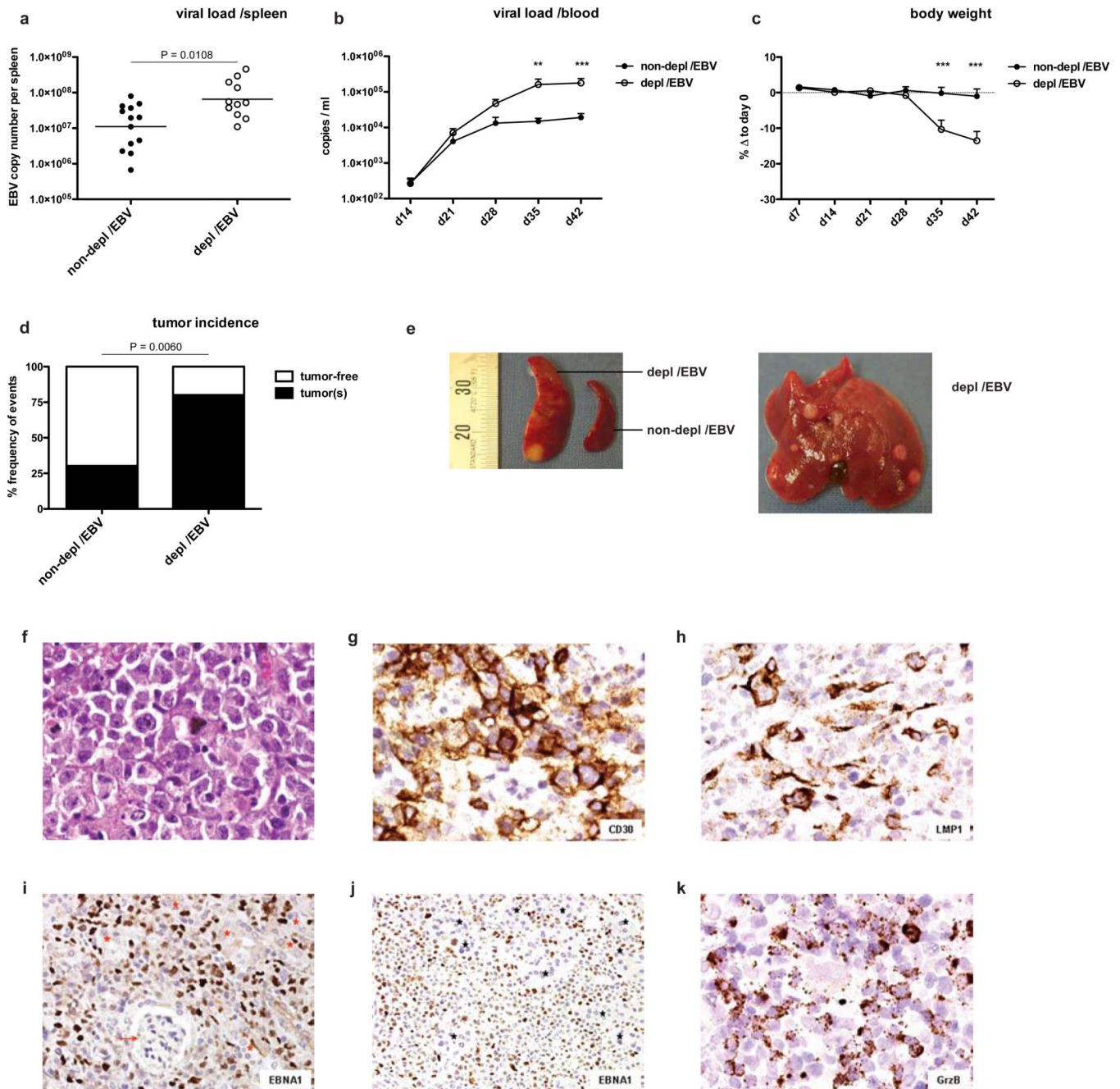


### Figure 3. NK cell-depleted animals develop increased viral titers and tumor burden after EBV infection

Viral titers in spleen six weeks after EBV infection in animals with (depl /EBV) and without (non-depl /EBV) NK cell depletion (**a**,  $n=24$ , horizontal bar represents geometric mean, two-tailed Mann Whitney test) and whole blood at various time points p.i. (**b**,  $n=21-26$  per time point, mean  $\pm$  s.e.m.,  $**P<0.01$ ,  $***P<0.001$ , two-way analysis of variance (ANOVA) with Bonferroni correction). **c**, percent body weight loss after EBV infection in animals with and without NK cell depletion at various time points p.i. relative to day 0 ( $n=15-26$  per time point, mean  $\pm$  s.e.m.,  $***P<0.001$ , two-way analysis of variance (ANOVA) with Bonferroni correction). **d**, incidence of all infiltrative tumors at multiple sites six weeks p.i. in animals

with and without NK cell depletion (n=36, Fisher's exact test for actual numbers). All data represent composite data from three to four independent experiments. **e**, spleen with and without tumor formation from NK cell-depleted or non-depleted animals six weeks p.i., respectively (left picture) and liver from NK cell-depleted animal with multiple tumors (right picture). **f–k**, tumor morphology. **f–h**, pleomorphic immunoblasts including occasional Reed-Sternberg like-cells (H&E) (**f**) and **g**, pleomorphic immunoblasts showing CD30 expression. **h**, EBV infected cells with expression of LMP1. Original magnification, 400×. **i** and **j**, EBNA1<sup>+</sup> (brown nuclear staining) pleomorphic immunoblasts in tumor bearing kidney (**i**, arrow indicates glomerulus and red stars indicate renal tubules) and pancreatic tumor (**j**, black stars indicate the pancreatic acini). Original magnification, 200×. **k**, spleen infiltrated by large numbers of granzyme B<sup>+</sup> cells (original magnification, 400×). All tissue derived from animals six weeks p.i.

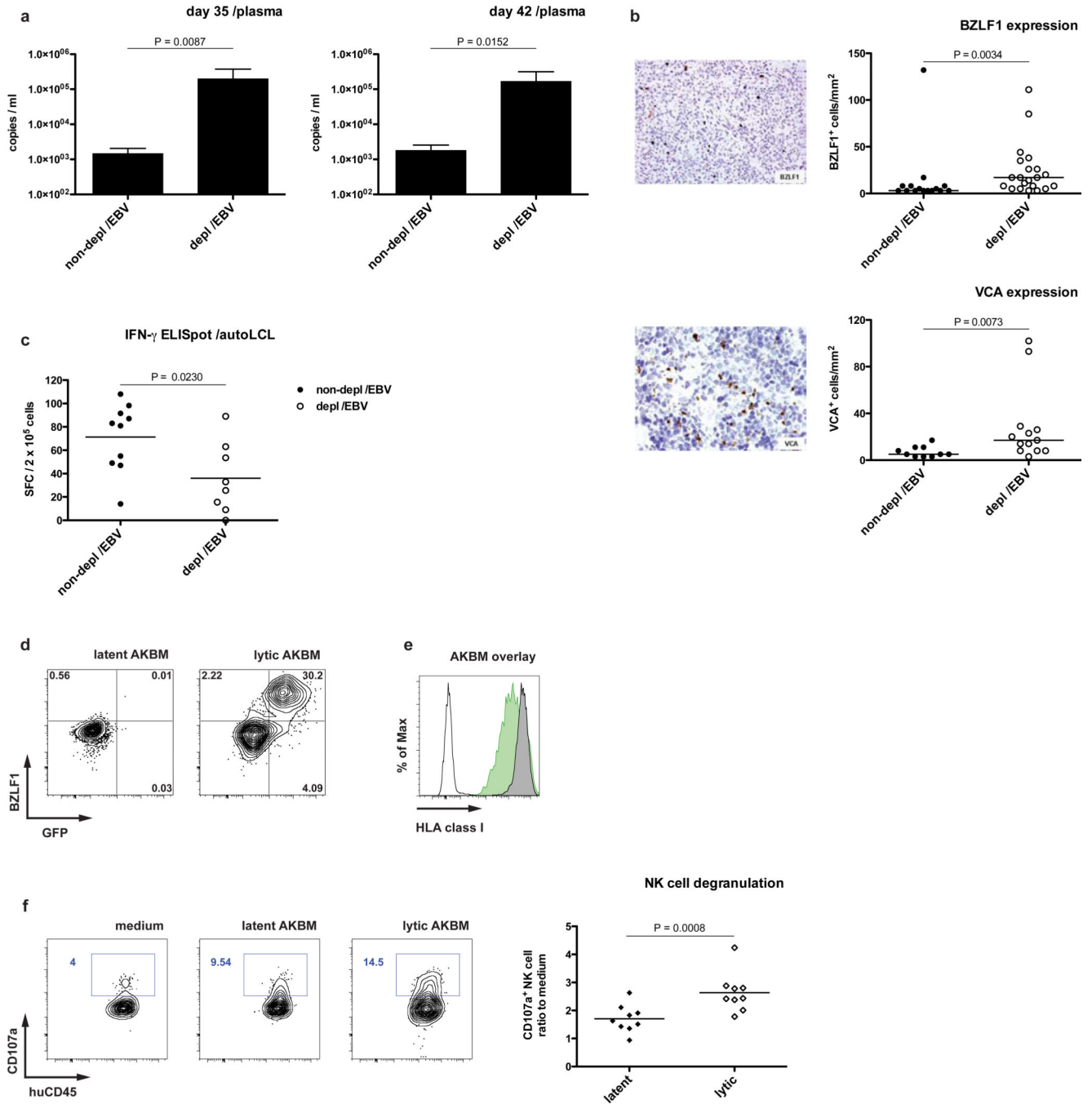


**Figure 4. Loss of NK cell mediated immune control augments lytic EBV infection**  
**a–b**, EBV wild-type infection. **a**, EBV genome copies in plasma five and six weeks p.i. in animals with (depl /EBV) and without (non-depl /EBV) NK cell depletion (n=11–12, mean  $\pm$  s.e.m., two-tailed Mann Whitney test). **b**, staining for BZLF-1 (upper left, original magnification, 200 $\times$ ) and VCA (lower left, original magnification, 400 $\times$ ) in splenic sections from NK cell-depleted animals six weeks p.i. with quantification of BZLF-1<sup>+</sup> cells per mm<sup>2</sup> in animals with and without NK cell depletion (upper right) and VCA<sup>+</sup> cells per mm<sup>2</sup> in animals with and without NK cell depletion (lower right), n=23–36, horizontal bars represent median, two-tailed Mann Whitney test. **c**, functional assay (IFN- $\gamma$  ELISpot) of ex

vivo T cell response six weeks p.i. with autologous LCLs as targets and effector CD19<sup>+</sup> depleted splenic cells from animals with and without NK cell depletion (E:T = 5:1). n=18, horizontal bar represents mean. **d–f**, induction of lytic phase in AKBM cells and NK cell response. Staining for BZLF-1 in latent and lytic (induced) AKBM cells versus BMRF-1 driven GFP expression (**d**). **e**, HLA class I expression in latent and lytic AKBM cells (latent: grey graph, lytic: green graph, white graph: unstained control). **f**, degranulation of pre-gated splenic NK cells from infected animals six weeks p.i. towards latent and lytic AKBM cells (n=9, horizontal bar represents mean). All data represent composite data from at least two independent experiments.

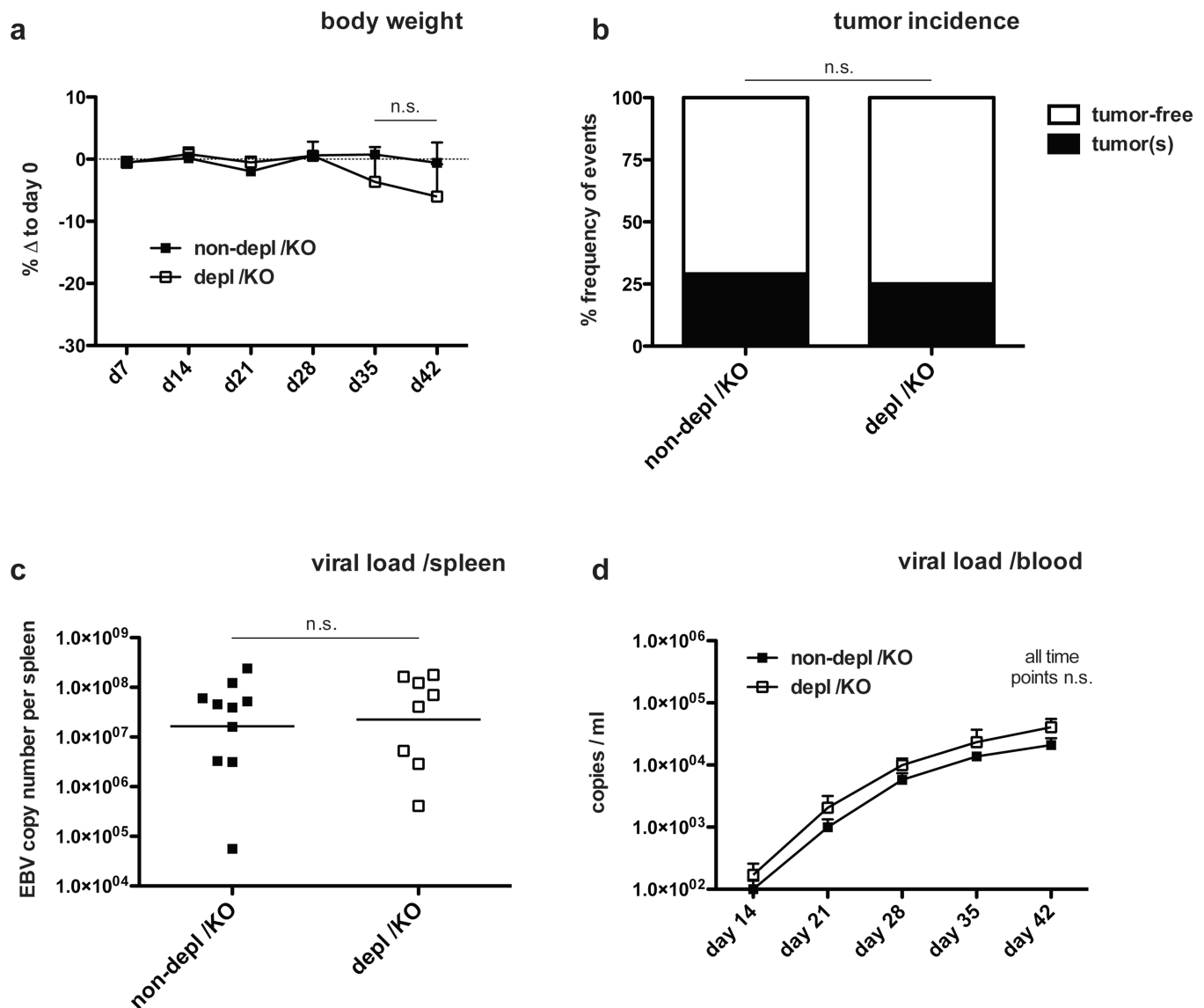


**Figure 5. Latent EBV infection is not affected by human NK cells**

**a–d**, EBV BZLF-1 KO infection. Body weight loss after EBV BZLF-1 KO infection in animals with (depl /KO) and without (non-depl /KO) NK cell depletion at various time points p.i. (**a**,  $n=12$ , mean  $\pm$  s.e.m., two-way analysis of variance (ANOVA) with Bonferroni correction). **b**, tumor incidence six weeks after EBV BZLF-1 KO infection in NK cell-depleted and non-depleted animals ( $n=15$ , Fisher's exact test for actual numbers). **c–d**, viral titers in spleen six weeks p.i. (**c**,  $n=18$ , horizontal bar represents geometric mean, two-tailed Mann Whitney test) and blood at various time points p.i. (**d**,  $n=12–18$ , mean  $\pm$  s.e.m., \* $P<0.05$ , two-way analysis of variance (ANOVA) with Bonferroni correction) in animals with and without NK cell depletion. All data represent composite data from at least two independent experiments.